



Obesity significantly alters the human sperm proteome, with potential implications for fertility

T. Pini¹ · J. Parks¹ · J. Russ¹ · M. Dzieciatkowska² · K. C. Hansen² · W. B. Schoolcraft¹ · M. Katz-Jaffe¹

Received: 3 October 2019 / Accepted: 30 January 2020 / Published online: 5 February 2020
© Springer Science+Business Media, LLC, part of Springer Nature 2020

Abstract

Purpose In men, obesity may lead to poor semen parameters and reduced fertility. However, the causative links between obesity and male infertility are not totally clear, particularly on a molecular level. As such, we investigated how obesity modifies the human sperm proteome, to elucidate any important implications for fertility.

Methods Sperm protein lysates from 5 men per treatment, classified as a healthy weight (body mass index (BMI) ≤ 25 kg/m²) or obese (BMI ≥ 30 kg/m²), were FASP digested, submitted to liquid chromatography tandem mass spectrometry, and compared by label-free quantification. Findings were confirmed for several proteins by qualitative immunofluorescence and a quantitative protein immunoassay.

Results A total of 2034 proteins were confidently identified, with 24 proteins being significantly ($p < 0.05$) less abundant (fold change < 0.05) in the spermatozoa of obese men and 3 being more abundant (fold change > 1.5) compared with healthy weight controls. Proteins with altered abundance were involved in a variety of biological processes, including oxidative stress (GSS, NDUFS2, JAGN1, USP14, ADH5), inflammation (SUGT1, LTA4H), translation (EIF3F, EIF4A2, CSNK1G1), DNA damage repair (UBE4A), and sperm function (NAPA, RNPEP, BANF2).

Conclusion These results suggest that oxidative stress and inflammation are closely tied to reproductive dysfunction in obese men. These processes likely impact protein translation and folding during spermatogenesis, leading to poor sperm function and subfertility. The observation of these changes in obese men with no overt andrological diagnosis further suggests that traditional clinical semen assessments fail to detect important biochemical changes in spermatozoa which may compromise fertility.

Keywords Obesity · Reproduction · Spermatozoa · Fertility · Proteome · LC-MS/MS

Introduction

Excessive body weight continues to be a growing problem in the twenty-first century; estimates of overweight and obesity (i.e., a body mass index (BMI) of ≥ 25 kg/m²) in adults remain high at 38.9% globally [1]. In the USA, 37.8% of men of

reproductive age (20–59 years) are obese (BMI ≥ 30 kg/m² [2]), highlighting that this population is at risk for experiencing co-morbidities of obesity. As the sequelae of excessive body weight have been investigated, it has become clear that obesity has significant negative implications for fertility. In men, this often manifests as poor semen parameters including below average sperm motility, concentration, and normal morphology [3–5]. In addition, obese men are significantly less likely to conceive naturally within 12 months of trying [6, 7]. Paternal obesity has further been shown to impact the fertility of the subsequent generation in rodent studies, with male offspring demonstrating poor semen parameters and reduced fertilization rates [8, 9]. These data emphasize the negative effects of obesity on male fertility, and highlight the need to further understand the mechanisms underlying these effects and investigate possible solutions.

While obesity is clearly linked to poor semen parameters, diagnosis of the latter remains centered around basic semen

Electronic supplementary material The online version of this article (<https://doi.org/10.1007/s10815-020-01707-8>) contains supplementary material, which is available to authorized users.

✉ T. Pini
tpini@fcoloro.com

¹ Colorado Center for Reproductive Medicine, Lone Tree, CO 80124, USA

² School of Medicine Biological Mass Spectrometry Facility, University of Colorado, Aurora, CO 80045, USA

assessment [10]. Assays evaluating basic parameters such as sperm motility, concentration, and morphology may fail to detect obesity-derived changes in spermatozoa operating at the molecular level. Previous studies support this idea, demonstrating that spermatozoa from obese men have altered abundances of a handful of proteins despite being largely normozoospermic (i.e., complying with World Health Organization standards for sperm motility, morphology, and concentration) [11, 12]. However, these studies employed two-dimensional difference gel electrophoresis (2D-DIGE), a proteomic method with good sensitivity, but limitations of low reproducibility, narrow dynamic range, and poor separation of highly hydrophobic or acidic/basic proteins [13]. In comparison, proteomic analysis of samples by liquid chromatography tandem mass spectrometry (LC-MS/MS) offers high sensitivity, with improvements in dynamic range and accurate analysis of proteins regardless of hydrophobicity or isoelectric point [14]. Combined with the use of label-free quantification, LC-MS/MS offers robust and reliable identification of proteomic differences in complex samples, including human spermatozoa [15]. While a previous study by Liu et al. [16] used LC-MS/MS to investigate the sperm proteome of obese men, this was limited to a small sample size ($n=3$ men), incorporated the complicating factor of severe asthenozoospermia and did not appear to control for relevant factors such as diabetes or smoking. In contrast, we sought to analyze clinically normal samples from a well-controlled population of obese men. Such a deep exploration of the human sperm proteome in the context of obesity could provide insight into the mechanistic links between obesity and infertility, as well as offering more information for clinical assessment of semen parameters, and potential pathways to improve semen quality.

In this context, we performed an in depth proteomic analysis of clinically normal human spermatozoa from healthy weight and obese men using LC-MS/MS. We present a comprehensive sperm proteome investigating the impacts of obesity on a molecular level and discern potential implications for male fertility.

Materials & methods

Chemicals

All chemicals were purchased from Sigma Aldrich (St Louis, MI) unless otherwise stated and were of HPLC grade. Antibodies used for immunofluorescence were purchased from Santa Cruz Biotechnology (Dallas, TX) and Thermo Fisher Scientific (Waltham, MA). Antibodies used for the quantitative protein immunoassay were purchased from Novus Biologicals (Centennial, CO).

Ethical approval

Semen was collected with consent from patients at the Colorado Center for Reproductive Medicine (Lone Tree, CO) and approval from the Western Institutional Review Board (Puyallup, WA, protocol number 20142468).

Patient selection, semen processing, and statistical analysis

Human semen was collected on the day of oocyte retrieval. Men were selected based on age (<50) and BMI (control = BMI <25 kg/m², obese = BMI >30 kg/m²). Patients were excluded if they smoked tobacco or had a history of diabetes, hypertension, testicular injuries, or other significant medical conditions. Only men with clinically normal semen were recruited; applied cut offs included semen concentration $>15 \times 10^6$ spermatozoa/mL, sperm motility $>20\%$, normal morphology (strict Kruger criteria [17]) $\geq 1\%$, and DNA fragmentation (terminal deoxynucleotidyl transferase (TdT) dUTP nick-end labeling (TUNEL) assay) $<16\%$ (if measured). Samples with significant somatic cell contamination were excluded. Routine clinical data, including age, BMI, semen concentration, motility, morphology, and DNA fragmentation, were subjected to statistical analysis by Student's two-tailed *t* test employing an α of 0.05. Values for sperm concentration and motility were obtained from the ejaculate used for proteomic analysis.

Ejaculates were collected by masturbation, allowed to liquefy, and separated on a 90%/45% PureSperm gradient (Nidacon) to remove somatic cells and isolate viable spermatozoa. Sperm pellets were washed twice with G-IVF (Vitrolife) supplemented with 5 mg/mL serum protein supplement (SAGE media) in preparation for intracytoplasmic sperm injection (ICSI). Following ICSI, surplus washed semen was either cryopreserved (proteome, $n=5$ men per treatment) or immediately underwent processing for qualitative immunofluorescence or the quantitative protein immunoassay as described below. For cryopreservation, washed ejaculates were centrifuged ($300 \times g$, 10 min) to remove G-IVF, resuspended 1:1 (v/v) in TEST-yolk buffer (12% (v/v) glycerol, 20% (v/v) egg yolk, 10 μ g/mL gentamicin sulfate, Irvine Scientific), and suspended in liquid nitrogen vapor for 20 min before immersion in liquid nitrogen. Samples were stored at -80 °C and thawed by shaking in a 37 °C water bath for 2 min prior to proteomic analysis.

Preparation of sperm cell lysates

Frozen thawed samples were further washed ($300 \times g$, 10 min, 2 \times) with Dulbecco's phosphate buffered saline (PBS, without calcium and magnesium, Gibco) to remove TEST-yolk buffer and any remaining serum protein supplement. Sperm pellets were resuspended in an equal volume of lysis buffer (10 mM tris, 2% (w/v) sodium dodecyl sulfate (SDS), cOmplete mini

EDTA free protease inhibitor cocktail) and incubated for 1 h at room temperature with regular vortexing. Lysates were centrifuged (7500×g, 15 min), and both the supernatant and pellet were retained. Cell pellets were solubilized in 200 µL 8 M urea, 100 mM ammonium bicarbonate (U-ABC), vortexed for 20 min, and centrifuged (14,000×g, 10 min). Both supernatants were snap frozen and stored at –80 °C until further processing.

FASP digestion

Samples were individually prepared for mass spectrometry using filter aided sample preparation (FASP). Cell lysate and solubilized pellet supernatant were combined for each sample, the mixture applied to a 30 kDa filter unit (Vivacon, Sartorius; pre-washed with U-ABC) containing 200 µL U-ABC, and centrifuged (14,000×g, 15 min). SDS was removed by 3 washes with 200 µL U-ABC (13,000×g, 15 min). Proteins were reduced (10 mM dithiothreitol, 30 min, room temperature) and alkylated (50 mM iodoacetamide, 30 min, room temperature, in the dark), washed with U-ABC and 50 mM ammonium bicarbonate and trypsin digested (sequencing grade modified trypsin, 1:50 enzyme:protein, in 0.02% (v/v) protease max/50 mM ammonium bicarbonate, 16 h at 37 °C). Peptides were washed and eluted with consecutive washes of 50 mM ammonium bicarbonate and 0.1% (v/v) formic acid (FA) (13,000×g, 10 min). Digested peptides were dried to minimum volume in a vacuum centrifuge, resuspended in 150 µL 0.5% (v/v) FA and applied to activated STAGE (STop and Go Extraction) tips [18] (activated with 80% (v/v) acetonitrile, 0.5% (v/v) FA, and equilibrated with 0.1% (v/v) FA) containing C18 resin (binding capacity ~10 µg). Samples were reapplied to tips 3 times to ensure saturation of resin (1500×g, 1 min) and washed (0.1% (v/v) FA, 1500×g, 2 min) to remove any remaining contaminants. Peptides were eluted (80% (v/v) acetonitrile, 0.5% (v/v) FA), dried to minimum volume in a vacuum centrifuge, and resuspended with 0.1% (v/v) FA prior to injection.

Liquid chromatography tandem mass spectrometry

All samples ($n = 5$ per treatment) were run in duplicate to account for any between-run variation. Samples were analyzed on a Q Exactive HF quadrupole orbitrap mass spectrometer (Thermo Fisher Scientific, Waltham, MA) coupled to an Easy nLC 1000 UHPLC (Thermo Fisher Scientific) through a nanoelectrospray ion source. Peptides were separated on a self-made C18 analytical column (100 µm internal diameter, ×20 cm length) packed with 2.7 µm Phenomenex Cortecs particles. After equilibration with 3 µL 5% (v/v) acetonitrile and 0.1% (v/v) formic acid, the peptides were separated by a 240-min linear gradient from 4% (v/v) to 30% (v/v) acetonitrile with 0.1% (v/v) formic acid at 400 nL/min. LC mobile phase solvents and sample dilutions used 0.1% (v/v) formic acid in water (buffer A) and 0.1% formic acid (v/v) in acetonitrile

(buffer B) (Optima™ LC/MS, Fisher Scientific, Pittsburgh, PA). Data acquisition was performed using the instrument supplied Xcalibur™ (v 4.0) software. The mass spectrometer was operated in the positive ion mode, in the data-dependent acquisition mode. Full MS scans were obtained with a range of m/z 300–1600, a mass resolution of 120,000 at m/z 200, and a target value of 1.00E+06 with the maximum injection time of 50 ms. HCD collision was performed on the 15 most significant peaks, and tandem mass spectra were acquired at a mass resolution of 30,000 at m/z 200 and a target value of 1.00E+05, with a maximum injection time of 100 ms. Isolation of precursors was performed with a window of 1.2 Th. The dynamic exclusion time was 20 s. The normalized collision energy was 32. Precursor ions with single, unassigned, or eight and higher charge states were excluded from fragmentation selection.

Protein identification

MS/MS spectra were extracted from raw data files and converted into Mascot generic files (.mgf) using Proteome Discoverer (v 2.2, Thermo Fisher Scientific). Mascot generic files were batch searched using an in-house Mascot server (v 2.6, Matrix Science), against the SwissProt database (release date February 2018, 20,333 entries), with taxonomy set to *Homo sapiens*. Search parameters included trypsin as the protease, allowing up to 1 missed cleavage, carbamidomethyl cysteine as a fixed modification, acetylation of N-terminal proteins, oxidation of methionine and proline, and N-terminal pyroglutamate as variable modifications, MS peak tolerance of 15 ppm, MS/MS fragment ion tolerance of 25 ppm, and peptide charges of 1+, 2+, and 3+ and #C13C of 1.

Label-free quantification of protein abundance and statistical analysis

Mascot .dat files were loaded into (v 4.8.9, Proteome Software Inc.) for ID validation and quantitative analysis. Peptide and protein identifications were accepted if they were established at greater than 95% or 99% probability by the Peptide Prophet [19] and Protein Profit [20] algorithms, respectively. Positive protein identifications also required a minimum of 2 unique peptides. Proteins that contained similar peptides and could not be differentiated based on MS/MS analysis alone were grouped to satisfy the principles of parsimony. False discovery rate (FDR) was calculated within Scaffold, using peptide and protein probabilities calculated by Peptide Prophet and Protein Profit algorithms. Quantitative comparisons employed normalized weighted spectra (NWS) using experiment-wide protein grouping, and treatment groups were compared using a Student's two-tailed t test within Scaffold, with an α of 0.05. Data were exported to Excel and ranked by fold change; only samples with a fold change of ≥ 1.5 or ≤ 0.5 were further considered as significant. To further enhance the validity of

the quantitative comparison, a minimum NWS cutoff of 5 was applied to the patient group with the highest abundance of each protein (i.e., NWS below 5 was accepted if present in the patient group with significantly reduced protein abundance).

Gene ontology and protein network interactions

Identified proteins were further characterized using PANTHER (www.pantherdb.org, v 14.0) for gene ontology and STRING (www.string-db.org, v 11.0) to identify protein network interactions. In both cases, species was specified as *Homo sapiens*.

Qualitative immunofluorescence

Qualitative immunofluorescence was performed to corroborate a representative selection of proteins which were significantly differentially abundant in the sperm proteome of obese men (GSS and NDUF52). Samples used for immunofluorescence were obtained from new cohorts of control and obese patients ($n = 3$ per treatment, under the same inclusion/exclusion criteria as previously stated) to ensure that findings could be generalized to a different population of patients. Fresh post-ICSI samples were washed ($300\times g$, 10 min) with PBS, diluted to 50×10^6 spermatozoa/mL, and gently smeared on poly-L-lysine-coated slides. Slides were air dried and stored at -20°C until use. Slides were allowed to warm to room temperature and fixed/permeabilized in 100% ice cold methanol for 1 min. Slides were blocked with 5% (v/v) goat serum in PBS and 0.1% (v/v) Tween 20 (PBST) for 60 min, then treated with primary antibody (1:50 dilution, Supplemental Table S1) diluted in 5% (v/v) goat serum in PBST for 1.5 h. Slides were washed 4 times for 5 min each in PBST, then incubated with a FITC-conjugated goat anti-mouse secondary antibody (1:100 dilution, Supplemental Table S1) diluted in 5% (v/v) goat serum in PBST for 1.5 h. Slides were washed 4 times for 5 min each in PBST, then mounted in Fluoroshield with DAPI and immediately imaged using an Olympus BX52 fluorescent microscope and Coolsnap HQ camera, running Metamorph software (v 7.7.0.0). All images were captured under a $\times 60$ objective, with a standardized exposure time (10 s), and a consistent display range was set for each target using ImageJ (v 1.52a). Target localization and signal strength were qualitatively assessed in all samples.

Orthogonal validation of differentially abundant proteins

A quantitative immunoassay was performed as orthogonal validation for a representative selection of proteins which were significantly differentially abundant in the sperm

proteome of obese men (ADH5, GSS, LTA4H). Samples used for the immunoassay were obtained from new cohorts of control and obese patients ($n = 5$ per treatment, under the same inclusion/exclusion criteria as previously stated) to ensure that findings could be generalized to a different population of patients. Fresh post-ICSI samples were washed ($300\times g$, 10 min) with PBS, the supernatant discarded, and the pellet snap frozen and stored at -80°C . Pellets were lysed as above, protein concentration assessed by Qubit assay (ThermoFisher), and lysates diluted to a standardized concentration (200 $\mu\text{g/mL}$ for LTA4H or 800 $\mu\text{g/mL}$ for ADH5, GSS) in $0.1\times$ sample buffer (Protein Simple). Relative protein amounts were quantified using the automated Jess Simple Western protein immunoassay (Protein Simple), employing capillary based separation and chemiluminescent detection according to manufacturer's directions. Briefly, samples were diluted with a fluorescent master mix containing DTT (final concentration 40 mM) and reduced (100°C , 10 min). Proteins were electrophoretically separated by size, labeled with primary and secondary antibodies (Supplemental Table S1), and imaged using chemiluminescence. Fluorescent internal standards were used for quality control, and within-capillary total protein normalization was performed to account for any differences in protein loading. In addition, both positive (HeLa or Jurkat cell lysates) and negative (HeLa or Jurkat cell lysates with no primary antibody) controls were included to confirm appropriate performance of each antibody. All samples were run in duplicate for each protein target ($n = 10$ replicates per treatment). Relative protein amounts were assessed using the corrected area of chemiluminescent peaks and analyzed by Student's two-tailed t test, with an α of 0.05.

Results

Clinical data

There were no significant differences between control and obese patients in terms of age, semen concentration, motility, normal morphology, or DNA fragmentation (Table 1). In all cases, patients were considered to have clinically normal semen according to cut offs described (Supplemental Table S2). Average BMI was significantly higher in the obese compared with the control group (33.0 ± 0.6 vs 23.9 ± 0.4 kg/m^2 , $p < 0.001$).

Identification of proteins by LC-MS/MS and general characterization

A total of 606, 078 peptides (FDR 0.52%) corresponding to 2034 proteins (FDR 0.00%) were identified in the combined control and obese datasets after applying confidence cut offs (peptide (95%) and protein confidence (99%)), minimum 2 unique peptides per protein, Supplemental Table S3). By

Table 1 Clinical data of patients providing ejaculated semen for LC-MS/MS analysis

Parameter	Control (BMI < 25)		Obese (BMI > 30)		P value
	Mean ± SEM	Range	Mean ± SEM	Range	
Age	38.2 ± 2.2	33–46	41.0 ± 2.1	35–46	0.379
Body mass index (kg/m ²)	23.9 ± 0.4	22.4–24.9	33.0 ± 0.6	31.2–34.7	0.000002
Semen concentration (spermatozoa/mL)	93.2 × 10 ⁶ ± 13.3 × 10 ⁶	69–137 × 10 ⁶	83.5 × 10 ⁶ ± 28.3 × 10 ⁶	18–189 × 10 ⁶	0.764
Total motility (%)	64.6 ± 0.1	42–77	59.8 ± 0.1	26–78	0.675
Normal morphology (%) ^a	3.0 ± 0.9	1–5	2.8 ± 0.6	1–4	0.856
DNA fragmentation (%) ^b	3.4 ± 2.5	0–13	3.3 ± 0.2	3–4	0.959

^aBased on Kruger classification [1], assessed on Diff Quik stained slides

^bBased on TUNEL assay using In Situ Cell Death Detection Kit (Roche Diagnostics), percentage of spermatozoa with DNA strand breaks (i.e., positive staining)

Highlighted to show a significant *p* value (i.e. less than 0.05)

manual comparison with published human proteomes [16, 21–24], the vast majority of these proteins have previously been identified in human spermatozoa (2019/2034, 99.3%). All proteomic data has been made publically available via PRIDE (project accession number PXD014849).

GO analysis of all identified proteins (Supplemental Table S4) showed that the molecular functions of most identified proteins fall under either catalytic activity (GO:0003824, 633 proteins, 30.5% of total) or binding (GO:0005488, 490 proteins, 23.6% of total). Over 80% of proteins were involved in the following biological processes: metabolic process (GO:0008152, 575 proteins, 27.7% of total), cellular component organization or biogenesis (GO:0071840, 333 proteins, 16.1% of total), localization (GO:0051179, 302 proteins, 14.6% of total), biological regulation (GO:0065007, 270 proteins, 13.0% of total), or cellular process (GO:0009987, 222 proteins, 10.7% of total). A wide range of protein classes were identified, with hydrolase (PC00121, 223 proteins, 10.8% of total), oxidoreductase (PC00176, 141 proteins, 6.8% of total), nucleic acid binding (PC00171, 134 proteins, 6.5% of total), transferase (PC00220, 130 proteins, 6.3% of total), cytoskeletal protein (PC00085, 108 proteins, 5.2% of total), and enzyme modulator (PC00095, 105 proteins, 5.1% of total) being the most common.

The 50 most abundant proteins included protein families such as tubulins, dyneins, and heat shock proteins. The major interaction categories of these highly abundant proteins revealed by STRING analysis included metabolic processes (glycolysis, oxidative phosphorylation, beta oxidation of fatty acids), histones, structural proteins, sperm motility, sperm capacitation, and fertilization.

Quantitative differences in the global sperm proteome of obese men

From a total of 2034 proteins, 27 had significantly different abundance in obese compared with control samples

(Supplemental Table S5). Of these 27 proteins, 3 were significantly more abundant in spermatozoa of obese men (fold change ≥ 1.5, *p* < 0.05), while 24 were significantly less abundant (fold change ≤ 0.5, *p* < 0.05) compared with control spermatozoa (Table 2). Proteins with the most significant fold changes included protein jagunal homolog 1 (JAGN1), NADH dehydrogenase [ubiquinone] iron-sulfur protein 2 (NDUFS2), leukotriene A-4 hydrolase (LTA4H), eukaryotic initiation factor 4A-II (EIF4A2), and glutathione synthetase (GSS).

Qualitative immunofluorescence

Qualitative immunofluorescence of representative proteins confirmed abundance changes observed by LC-MS/MS (Fig. 1). GSS showed very strong signal in control spermatozoa, mostly restricted to the equatorial and post acrosomal region, while spermatozoa from obese men displayed only weak signal. NDUFS2 showed moderate signal in spermatozoa from obese men, as both an equatorial band, post acrosomal and midpiece staining, and control spermatozoa showed only dim signal with similar localization.

Orthogonal validation by quantitative protein immunoassay

Changes in protein abundance of ADH5, GSS, and LTA4H were confirmed by orthogonal validation using a Jess Simple Western protein immunoassay (Supplemental figure 1). Both ADH5 and GSS were confirmed to be significantly less abundant in spermatozoa of obese patients compared with controls (ADH5 control 66,160 ± 7641 vs obese 31,855 ± 4666 arbitrary units, *p* = 0.001; GSS control 175,907 ± 13,420 vs obese 107,161 ± 14,068 arbitrary units, *p* = 0.002). While the 63 kDa isoform of LTA4H was similar between control and obese patients, the 73 kDa isoform was significantly less

Table 2 Proteins identified by LC-MS/MS with significantly different abundance (by normalized weighted spectra) in spermatozoa from control (BMI < 25) vs obese (BMI > 30) men

Gene symbol	Protein name	Mean control	Mean obese	<i>p</i> value	Fold change (obese/control)
JAGN1	Protein jagunal homolog 1	4.87	8.46	0.04	1.7
NDUFS2	NADH dehydrogenase [ubiquinone] iron-sulfur protein 2, mitochondrial	13.85	21.53	0.00052	1.6
NUP35	Nucleoporin NUP53	20.39	31.10	0.041	1.5
BANF2	Barrier-to-autointegration factor-like protein	16.36	8.88	0.031	0.5
MPC1	Mitochondrial pyruvate carrier 1	11.76	5.34	0.027	0.5
USP14	Ubiquitin carboxyl-terminal hydrolase 14	10.65	4.98	0.016	0.5
RAB18	Ras-related protein Rab-18	8.09	3.77	0.042	0.5
EIF3F	Eukaryotic translation initiation factor 3 subunit F	7.49	3.58	0.039	0.5
SUGT1	Protein SGT1 homolog	16.20	6.87	0.017	0.4
FAHD2A	Fumarylacetoacetate hydrolase domain-containing protein	8.50	3.45	0.026	0.4
CCDC189	Coiled-coil domain-containing protein 189	8.06	3.43	0.0031	0.4
ADH5	Alcohol dehydrogenase class-3	13.62	6.09	<0.0001	0.4
CSNK1G1	Casein kinase I isoform gamma-1	13.41	4.48	0.012	0.3
NAPA	Alpha-soluble NSF attachment protein	8.50	2.45	0.0017	0.3
KIAA1324	UPF0577 protein KIAA1324	7.20	2.10	0.005	0.3
UBE4A	Ubiquitin conjugation factor E4 A	6.19	2.08	0.011	0.3
NT5C	5'(3')-deoxyribonucleotidase, cytosolic type	6.33	1.98	0.028	0.3
SKP1	S-phase kinase-associated protein 1	6.22	1.79	0.026	0.3
LRRC74A	Leucine-rich repeat-containing protein 74A	10.37	2.01	0.0013	0.2
TTC12	Tetratricopeptide repeat protein 12	8.87	1.86	0.012	0.2
ATIC	Bifunctional purine biosynthesis protein PURH	6.73	1.55	0.0021	0.2
C1orf100	Uncharacterized protein C1orf100	6.35	1.06	0.0022	0.2
GLOD4	Glyoxalase domain-containing protein 4	6.76	1.08	<0.0001	0.2
RNPEP	Aminopeptidase B	7.52	0.68	0.0053	0.09
GSS	Glutathione synthetase	5.81	0.53	0.00019	0.09
EIF4A2	Eukaryotic initiation factor 4A-II	5.11	0.43	0.0048	0.08
LTA4H	Leukotriene A-4 hydrolase	5.09	0.37	0.00079	0.07

abundant in spermatozoa of obese men (control $126,432 \pm 4737$ vs obese $93,436 \pm 8151$ arbitrary units, $p = 0.003$).

Discussion

Using LC-MS/MS, we identified 27 proteins which are significantly different in abundance in the spermatozoa of obese men compared with men of a healthy weight. These results demonstrate that excessive body weight has implications in the male reproductive tract, leading to significant alterations in the sperm proteome. We believe that these alterations are truly a reflection of obesity, as patient cohorts did not differ in any other relevant factors (e.g., age, semen parameters, tobacco use), and patients with complicating factors (e.g., diabetes, oligozoospermia) were excluded. Interestingly, while clinical semen analysis showed no significant differences in semen parameters, mass spectrometric analysis demonstrated significant changes to the

sperm proteome, suggesting that even obese men with no severe andrological pathologies may have important molecular alterations to their spermatozoa. The proteomic data gathered in this study suggest possible mechanisms by which the spermatozoa of obese men may be negatively impacted (Fig. 2).

Proteins with altered abundance in the spermatozoa of obese men are involved in a diverse range of processes, yet their common roles serve to highlight how obesity may impact both spermatogenesis and mature sperm function. While mature spermatozoa are thought to be largely transcriptionally silent, changes in protein abundance while spermatozoa are fully transcriptionally active (i.e., during spermatogenesis) are likely to have wide ranging and significant impacts. Several proteins with decreased abundance in spermatozoa from obese men had important roles in transcription and translation, including the eukaryotic translation initiation factors EIF3F and EIF4A2. EIF3F is a subunit of the eIF3 complex, which is involved in mRNA recruitment to initiate protein synthesis.

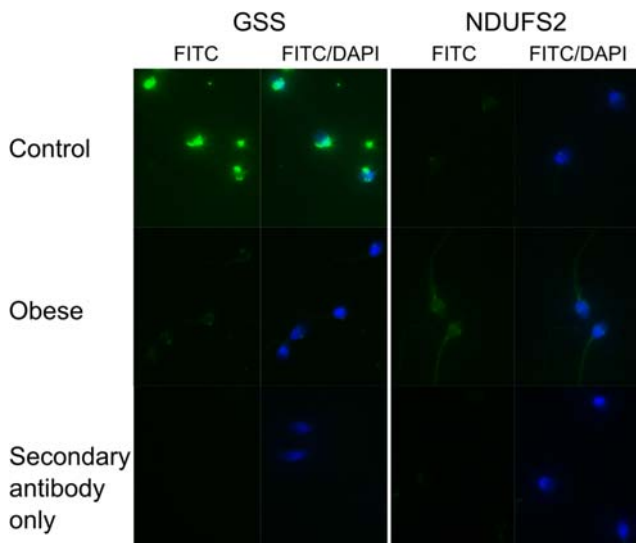


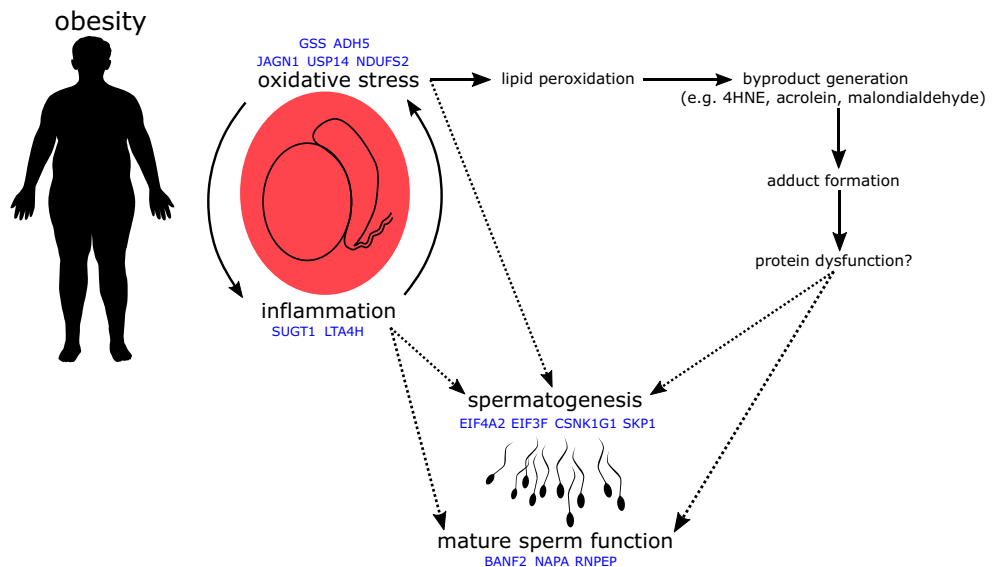
Fig. 1 Representative images of qualitative immunofluorescence. Spermatozoa from control (BMI < 25 kg/m²) or obese (BMI > 30 kg/m²) men were incubated with antibodies against GSS or NDUFS2 and a FITC-conjugated secondary antibody. DAPI staining was included to identify all spermatozoa. A secondary antibody only control was included to assess non-specific binding

EIF3F specifically inhibits protein synthesis at the translational level [25], and the decreased expression of this protein in cancer cells protects them from apoptosis [26]. In comparison, EIF4A2 is involved in mRNA silencing via micro RNAs [27]. Expression of casein kinase 1 gamma 1 (CSNK1G1) was also decreased; it is a prolific signaling molecule, involved in hedgehog, NFκB, p53, PI3K/AKT, and Wnt signaling cascades [28], all of which impact transcription and translation of their various downstream targets. The observed reduced abundance of these regulators of transcription and translation demonstrates that obesity may have significant implications for gene expression during spermatogenesis.

Obesity creates a chronic inflammatory state in the body, driven by interactions between adipose tissue and the immune system [29]. This inflammatory state undoubtedly impacts the testes, where increased levels of pro-inflammatory cytokines, inflammation markers, and macrophage infiltration are observed as a result of chronic obesity [30–33]. Inflammation occurring in the testes of obese men may be reflected in, and to some extent explained by, the proteomic alterations we observed. We found reduced levels of SUGT1 (alias SGT1), a co-chaperone of HSP90 with roles in Akt signaling [34], centromere function [35], and regulation of NLRP3 inflammasomes [36]. Obesity is associated with increased expression of NLRP3 [37], and as the SUGT1-HSP90 complex is responsible for maintaining these inflammasomes in a repressed state, limited levels of SUGT1 could potentially lead to an aberrant immune response and auto-activation of inflammatory pathways [36]. Interestingly, leukotriene A4 hydrolase (LTA4H) was also reduced in abundance in the spermatozoa of obese men. LTA4H has both pro- and anti-inflammatory roles, catalyzing the production of the pro-inflammatory mediator leukotriene B4 and degrading the chemoattractant peptide PGP [38]. Due to its potent capacity for degrading PGP, reduced abundance of this protein could help to sustain local inflammation in the testes. Interestingly, both the production and activity of LTA4H is reduced by acrolein [39], a byproduct of lipid peroxidation, which could be produced by developing spermatozoa undergoing oxidative stress [40]. While inflammation associated with obesity is primarily propelled by adipose tissue, reduced levels of SUGT1 and LTA4H could help to maintain inflammation in the testes of obese men.

Chronic low level inflammation contributes to oxidative stress, another significant side effect of obesity [41]. This state of oxidative stress is again locally observed in the testes of obese males, reflected by higher concentrations of both reactive

Fig. 2 Obesity creates systemic inflammation and oxidative stress, two closely inter-related processes. When occurring locally in the testes, these processes may impact spermatogenesis and mature sperm function either directly, or indirectly, via the formation of protein/reactive byproduct adducts and subsequent protein dysfunction



oxygen species (ROS) in spermatozoa [5, 42, 43] and products of lipid peroxidation in testicular tissues [44–46]. These products of lipid peroxidation (e.g., 4HNE, acrolein, malondialdehyde) cause further problems by forming protein adducts which may alter protein structure and function, potentially in a deleterious manner [47]. Only 3 proteins were observed at a higher abundance in the spermatozoa of obese men, and 2 of these, NDUFS2 and JAGN1, may have important interactions with oxidative stress and its corollaries. NDUFS2, a component of mitochondrial complex I, forms adducts with lipid peroxidation products under conditions of oxidative stress [48, 49], potentially modifying its structure and/or function and causing mitochondrial dysfunction. Such an alteration could help to explain increases in mitochondrial ROS production [50] and the aberrant mitochondrial function observed in the spermatozoa of obese men [51, 52]. The heightened expression of JAGN1 observed in spermatozoa is likely due to induction of the unfolded protein response during spermatogenesis as a result of endoplasmic reticulum (ER) stress [53], a commonly observed side effect of obesity, driven in part by oxidative stress [54]. We also observed a reduction in USP14, a proteasome-associated deubiquitinating enzyme, which ties together both oxidative and ER stress. Inhibition of USP14 increases degradation of proteins adducted by lipid peroxidation byproducts, enhancing cellular resistance to oxidative stress [55]. In addition, silencing of USP14 activates the ER-associated degradation pathway, increasing breakdown of unfolded proteins in the ER [56]. USP14 was similarly found to be decreased in spermatozoa of obese, asthenozoospermic men [16]. Thus, while increased levels of NDUFS2 and JAGN1 may be causes and symptoms of oxidative stress, reduced levels of USP14 may be a mechanism for coping with oxidative stress, by allowing for increased breakdown of protein adducts and clearance of unfolded proteins.

The loss of antioxidant capacity is another hallmark of obesity [57]. The tripeptide thiol antioxidant glutathione has been found at reduced levels in serum and various body tissues of obese individuals [58–60]. Of note, low glutathione levels have also been observed in the semen of men with various infertility diagnoses [61, 62]. Intriguingly, we saw reduced levels of glutathione synthetase (GSS), which catalyzes the final step of glutathione synthesis. Reduced availability of GSS may directly limit glutathione synthesis, leaving spermatozoa from obese men vulnerable to oxidative damage. We also observed significantly decreased levels of ADH5 (alias GSNOR) in spermatozoa from obese men. ADH5 maintains the balance of GNSO formation and protein nitrosylation, without producing reactive intermediates or end products, thus representing a significant element of cellular antioxidant defense [63]. This activity of ADH5 also contributes to the maintenance of an intracellular glutathione pool; thus, the combined effect of reduced abundance of both GSS and ADH5 may significantly weaken glutathione-based antioxidant defenses in spermatozoa from obese men.

Several proteins which were less abundant in the spermatozoa of obese men compared with men of a healthy weight have important roles in a mature sperm function. NSF attachment protein alpha (NAPA, alias alpha-SNAP) plays a direct and indispensable role in the acrosome reaction [64, 65]. While NAPA is shed from the acrosome during exocytosis, anti-NAPA antibodies limit sperm-zona pellucida binding, suggesting that NAPA may also play a role in zona recognition and binding [66]. Aminopeptidase B (RNPEP, alias APB) is an exopeptidase which cleaves pro-neuropeptides into their active forms [67], and has previously been identified in the sperm acrosome [68]. Interestingly, both the pro-neuropeptide pro-enkephalin and its cleavage product met-enkephalin have also been detected in the human sperm head, and met-enkephalin has been shown to have significant positive effects on sperm motility [69]. While no direct links between RNPEP and the processing of pro-enkephalin in spermatozoa have been described, there is a strong possibility that this may be the exopeptidase responsible. In addition to sperm motility, RNPEP may also impact zona recognition; its inhibition in *Xenopus laevis* spermatozoa reduced vitelline membrane binding by 50% [70]. Barrier to autointegration factor 2 (BANF2, alias BAF-L) is a nuclear protein which, along with BANF1, is expressed in spermatids and retained in mature ejaculated spermatozoa, unlike many other nuclear proteins [71, 72]. BANF2 is highly expressed in the testes and is proposed to regulate the function of BANF1, which has roles in chromatin structure, segregation, and post-mitotic nuclear assembly [73]. These characteristics suggest that BANF2 may be important for maintaining nuclear shape in mature spermatozoa and formation of the male pro-nucleus following fertilization [72]. The reduced levels of NAPA, RNPEP, and BANF2 we observed could help to explain why obese males exhibit poor sperm motility, a deficient response to acrosome challenge [74, 75], reduced zona pellucida binding [76], and slower pronuclear fusion to achieve syngamy following fertilization [77].

Conclusion

We have shown that obesity significantly impacts the human sperm proteome, potentially to the detriment of important spermatogenic processes and the function of mature spermatozoa. These changes may be both symptoms of and contributors to the inflammation and oxidative stress associated with obesity, and may help to explain why obese men may have altered semen parameters, potentially leading to altered fertility. It is noteworthy that these changes were detected in obese men with no significant andrological diagnoses, indicating the failure of traditional clinical semen assessment to recognize molecular changes which could potentially compromise fertility. While some of the problems created by paternal obesity

may be overcome by ART, the swathe of implications following fertilization remains to be rigorously investigated. In addition, efforts should be directed toward the implementation of treatments to correct or limit the observed changes when weight loss prior to conception is neither practical nor realistic.

Acknowledgments The authors thank patients for their generous donation of samples.

Authors' roles T. Pini contributed to the experimental design, sample preparation, data acquisition, data analysis, drafting, and revision of the manuscript. J. Parks and J. Russ contributed to sample preparation. M. Dzieciatkowska and K.C. Hansen contributed to data acquisition and data analysis. W.B. Schoolcraft and M. Katz-Jaffe contributed to the experimental design. All authors critically revised the manuscript and gave final approval for publication.

Funding information This project was fully funded by the Colorado Center for Reproductive Medicine.

Compliance with ethical standards

Conflict of interest The authors declare that they have no conflicts of interest.

Ethical approval All procedures performed in studies involving human participants were in accordance with the ethical standards of the research committee (Western Institutional Review Board, protocol number 20142468) and with the 1964 Helsinki declaration and its later amendments or comparable ethical standards. Informed consent was obtained from all individual participants included in the study.

References

1. Organization WH. Prevalence of overweight among adults, BMI \geq 25, age-standardized, estimates by WHO region. Global Health Observatory data repository. 2017.
2. Hales C, Carroll M, Fryar C, Ogden C. Prevalence of obesity among adults and youth: United States, 2015–2016: National Center for Health Statistics 2017 Contract No.: 288.
3. Oliveira JBA, Petersen CG, Mauri AL, Vagnini LD, Renzi A, Petersen B, et al. Association between body mass index and sperm quality and sperm DNA integrity. A large population study. *Andrologia*. 2018;50(3):e12889.
4. Ramaraju GA, Teppala S, Prathigudupu K, Kalagara M, Thota S, Kota M, et al. Association between obesity and sperm quality. *Andrologia*. 2018;50(3):e12888.
5. Taha EA, Sayed SK, Gaber HD, Abdel Hafez HK, Ghandour N, Zahran A, et al. Does being overweight affect seminal variables in fertile men? *Reprod BioMed Online*. 2016;33(6):703–8.
6. Ramlau-Hansen CH, Thulstrup AM, Nohr EA, Bonde JP, Sørensen TIA, Olsen J. Subfecundity in overweight and obese couples. *Hum Reprod*. 2007;22(6):1634–7.
7. Sallmén M, Sandler DP, Hoppin JA, Blair A, Baird DD. Reduced fertility among overweight and obese men. *Epidemiology*. 2006;17(5):520–3.
8. McPherson NO, Fullston T, Bakos HW, Setchell BP, Lane M. Obese father's metabolic state, adiposity, and reproductive capacity indicate son's reproductive health. *Fertil Steril*. 2014;101(3):865–73.e1.
9. Fullston T, Palmer NO, Owens JA, Mitchell M, Bakos HW, Lane M. Diet-induced paternal obesity in the absence of diabetes diminishes the reproductive health of two subsequent generations of mice. *Hum Reprod*. 2012;27(5):1391–400.
10. Kliesch S. Diagnosis of male infertility: diagnostic work-up of the infertile man. *Eur Urol Suppl*. 2014;13(4):73–82.
11. Kriegel TM, Heidenreich F, Kettner K, Pursche T, Hoflack B, Grunewald S, et al. Identification of diabetes- and obesity-associated proteomic changes in human spermatozoa by difference gel electrophoresis. *Reprod BioMed Online*. 2009;19(5):660–70.
12. Paasch U, Heidenreich F, Pursche T, Kuhlisch E, Kettner K, Grunewald S, et al. Identification of increased amounts of eppin protein complex components in sperm cells of diabetic and obese individuals by difference gel electrophoresis. *Mol Cell Proteomics*. 2011;10(8):M110.
13. Magdeldin S, Enany S, Yoshida Y, Xu B, Zhang Y, Zureena Z, et al. Basics and recent advances of two dimensional- polyacrylamide gel electrophoresis. *Clin Proteomics*. 2014;11(1):16.
14. Feugang JM, Liao SF, Willard ST, Ryan PL. In-depth proteomic analysis of boar spermatozoa through shotgun and gel-based methods. *BMC Genomics*. 2018;19(1):62.
15. Codina M, Estanyol JM, Fidalgo MJ, Balleascà JL, Oliva R. Advances in sperm proteomics: best-practise methodology and clinical potential. *Expert Rev Proteomics*. 2015;12(3):255–77.
16. Liu Y, Guo Y, Song N, Fan Y, Li K, Teng X, et al. Proteomic pattern changes associated with obesity-induced asthenozoospermia. *Andrology*. 2015;3(2):247–59.
17. Kruger TF, Menkveld R, Stander FSH, Lombard CJ, Van Der Merwe JP, van Zyl JA, et al. Sperm morphologic features as a prognostic factor in in vitro fertilization. *Fertil Steril*. 1986;46(6):1118–23.
18. Rappsilber J, Ishihama Y, Mann M. Stop and go extraction tips for matrix-assisted laser desorption/ionization, nanoelectrospray, and LC/MS sample pretreatment in proteomics. *Anal Chem*. 2003;75(3):663–70.
19. Keller A, Nesvizhskii AI, Kolker E, Aebersold R. Empirical statistical model to estimate the accuracy of peptide identifications made by MS/MS and database search. *Anal Chem*. 2002;74(20):5383–92.
20. Nesvizhskii AI, Keller A, Kolker E, Aebersold R. A statistical model for identifying proteins by tandem mass spectrometry. *Anal Chem*. 2003;75(17):4646–58.
21. Amaral A, Castillo J, Ramalho-Santos J, Oliva R. The combined human sperm proteome: cellular pathways and implications for basic and clinical science. *Hum Reprod Update*. 2014;20(1):40–62.
22. Zhou T, Wang G, Chen M, Zhang M, Guo Y, Yu C, et al. Comparative analysis of macaque and human sperm proteomes: insights into sperm competition. *Proteomics*. 2015;15(9):1564–73.
23. Bogle OA, Kumar K, Attardo-Parrinello C, Lewis SEM, Estanyol JM, Balleascà JL, et al. Identification of protein changes in human spermatozoa throughout the cryopreservation process. *Andrology*. 2017;5(1):10–22.
24. Schiza C, Korbakis D, Jarvi K, Diamandis EP, Drabovich AP. Identification of TEX101-associated proteins through proteomic measurement of human spermatozoa homozygous for the missense variant rs35033974. *Mol Cell Proteomics*. 2019;18(2):338–51.
25. Marchione R, Leibovitch S, Lenormand J-L. The translational factor eIF3f: the ambivalent eIF3 subunit. *Cell Mol Life Sci*. 2013;70(19):3603–16.
26. Shi J, Kahle A, Hershey JWB, Honchak BM, Warneke JA, Leong SPL, et al. Decreased expression of eukaryotic initiation factor 3f deregulates translation and apoptosis in tumor cells. *Oncogene*. 2006;25:4923.
27. Meijer HA, Kong YW, Lu WT, Wilczynska A, Spriggs RV, Robinson SW, et al. Translational repression and eIF4A2 activity

- are critical for microRNA-mediated gene regulation. *Science*. 2013;340(6128):82–5.
28. Schitteck B, Sinnberg T. Biological functions of casein kinase I isoforms and putative roles in tumorigenesis. *Mol Cancer*. 2014;13(1):231.
 29. de Heredia FP, Gómez-Martínez S, Marcos A. Obesity, inflammation and the immune system. *Proc Nutr Soc*. 2012;71(2):332–8.
 30. Xiang J, Bian C, Wan X, Zhang Q, Huang S, Wu D. Sleeve gastrectomy reversed obesity-induced hypogonadism in a rat model by regulating inflammatory responses in the hypothalamus and testis. *Obes Surg*. 2018;28(8):2272–80.
 31. Huang G, Yuan M, Zhang J, Li J, Gong D, Li Y, et al. IL-6 mediates differentiation disorder during spermatogenesis in obesity-associated inflammation by affecting the expression of Zfp637 through the SOCS3/STAT3 pathway. *Sci Rep*. 2016;6:28012.
 32. Fan W, Xu Y, Liu Y, Zhang Z, Lu L, Ding Z. Obesity or overweight, a chronic inflammatory status in male reproductive system, leads to mice and human subfertility. *Front Physiol*. 2018;8:1117.
 33. Wagner IV, Klötting N, Atanassova N, Savchuk I, Spröte C, Kiess W, et al. Prepubertal onset of obesity negatively impacts on testicular steroidogenesis in rats. *Mol Cell Endocrinol*. 2016;437:154–62.
 34. Gao G, Kun T, Sheng Y, Qian M, Kong F, Liu X, et al. SGT1 regulates Akt signaling by promoting beta-TrCP-dependent PHLPP1 degradation in gastric cancer cells. *Mol Bio Rep*. 2013;40(4):2947–53.
 35. Niikura Y, Kitagawa R, Ogi H, Kitagawa K. SGT1-HSP90 complex is required for CENP-A deposition at centromeres. *Cell Cycle*. 2017;16(18):1683–94.
 36. Mayor A, Martinon F, De Smedt T, Pétrilli V, Tschopp J. A crucial function of SGT1 and HSP90 in inflammasome activity links mammalian and plant innate immune responses. *Nat Immunol*. 2007;8(5):497–503.
 37. Rheinheimer J, de Souza BM, Cardoso NS, Bauer AC, Crispim D. Current role of the NLRP3 inflammasome on obesity and insulin resistance: a systematic review. *Metab - Clin Exp*. 2017;74:1–9.
 38. Snelgrove RJ, Jackson PL, Hardison MT, Noerager BD, Kinloch A, Gaggar A, et al. A critical role for LTA4H in limiting chronic pulmonary neutrophilic inflammation. *Science*. 2010;330(6000):90–4.
 39. Noerager BD, Xu X, Davis VA, Jones CW, Okafor S, Whitehead A, et al. A potential role for acrolein in neutrophil-mediated chronic inflammation. *Inflammation*. 2015;38(6):2279–87.
 40. Bromfield EG, Aitken RJ, McLaughlin EA, Nixon B. Proteolytic degradation of heat shock protein A2 occurs in response to oxidative stress in male germ cells of the mouse. *Mol Hum Reprod*. 2017;23(2):91–105.
 41. Vincent HK, Taylor AG. Biomarkers and potential mechanisms of obesity-induced oxidant stress in humans. *Int J Obes*. 2005;30:400.
 42. Tunc O, Tremellen K. Oxidative DNA damage impairs global sperm DNA methylation in infertile men. *J Assisted Reprod Genet*. 2009;26(9):537–44.
 43. Fullston T, Shehadeh H, Sandeman LY, Kang WX, Wu LL, Robker RL, et al. Female offspring sired by diet induced obese male mice display impaired blastocyst development with molecular alterations to their ovaries, oocytes and cumulus cells. *J Assisted Reprod Genet*. 2015;32(5):725–35.
 44. Alhashem F, Alkhateeb M, Sakr H, Alshahrani M, Alsunaidi M, Elrefaey H, et al. Exercise protects against obesity induced semen abnormalities via downregulating stem cell factor, upregulating Ghrelin and normalizing oxidative stress. *EXCLI J*. 2014;13:551–72.
 45. Gujjala S, Putakala M, Gangarapu V, Nukala S, Bellamkonda R, Ramaswamy R, et al. Protective effect of *Caralluma fimbriata* against high-fat diet induced testicular oxidative stress in rats. *Biomed Pharmacother*. 2016;83:167–76.
 46. Atilgan D, Parlaktas BS, Uluocak N, Erdemir F, Kilic S, Erkorkmaz U, et al. Weight loss and melatonin reduce obesity-induced oxidative damage in rat testis. *Adv Urol*. 2013;2013:6.
 47. Barnes S, Shonsey Erin M, Eliuk Shannon M, Stella D, Barrett K, Srivastava Om P, et al. High-resolution mass spectrometry analysis of protein oxidations and resultant loss of function. *Biochem Soc Trans*. 2008;36(5):1037–44.
 48. Zhao Y, Miriyala S, Miao L, Mitov M, Schnell D, Dhar SK, et al. Redox proteomic identification of HNE-bound mitochondrial proteins in cardiac tissues reveals a systemic effect on energy metabolism after doxorubicin treatment. *Free Radic Biol Med*. 2014;72:55–65.
 49. Wen J-J, Garg N. Oxidative modification of mitochondrial respiratory complexes in response to the stress of *Trypanosoma cruzi* infection. *Free Radic Biol Med*. 2004;37(12):2072–81.
 50. de Mello AH, Costa AB, Engel JDG, Rezin GT. Mitochondrial dysfunction in obesity. *Life Sci*. 2018;192:26–32.
 51. Fariello RM, Pariz JR, Spaine DM, Cedenho AP, Bertolla RP, Fraietta R. Association between obesity and alteration of sperm DNA integrity and mitochondrial activity. *BJU Int*. 2012;110(6):863–7.
 52. Vignera S, Condorelli Rosita A, Vicari E, Calogero AE. Negative effect of increased body weight on sperm conventional and non-conventional flow cytometric sperm parameters. *J Androl*. 2013;33(1):53–8.
 53. Nosak C, Silva PN, Sollazzo P, Kyung-Mee M, Odisho T, Foster LJ, et al. JAGN1 is induced in response to ER stress and regulates proinsulin biosynthesis. *PLoS One*. 2016;11(2).
 54. Tripathi YB, Pandey V. Obesity and endoplasmic reticulum (ER) stresses. *Front Immunol*. 2012;3:240.
 55. Lee B-H, Lee MJ, Park S, Oh D-C, Elsasser S, Chen P-C, et al. Enhancement of proteasome activity by a small-molecule inhibitor of USP14. *Nature*. 2010;467:179–86.
 56. Nagai A, Kadowaki H, Maruyama T, Takeda K, Nishitoh H, Ichijo H. USP14 inhibits ER-associated degradation via interaction with IRE1 α . *Biochem Biophys Res Commun*. 2009;379(4):995–1000.
 57. Fernández-Sánchez A, Madrigal-Santillán E, Bautista M, Esquivel-Soto J, Morales-González Á, Esquivel-Chirino C, et al. Inflammation, oxidative stress, and obesity. *Int J Mol Sci*. 2011;12(5).
 58. Norris KM, Okie W, Kim WK, Adhikari R, Yoo S, King S, et al. A high-fat diet differentially regulates glutathione phenotypes in the obesity-prone mouse strains DBA/2J, C57BL/6J, and AKR/J. *Nutr Res*. 2016;36(12):1316–24.
 59. Ozaydin A, Onaran I, Yesim TE, Sargin H, Avsar K, Sultuybek G. Increased glutathione conjugate transport: a possible compensatory protection mechanism against oxidative stress in obesity? *Int J Obes*. 2006;30(1):134–40.
 60. Pastore A, Ciampalini P, Tozzi G, Pecorelli L, Passarelli C, Bertini E, et al. All glutathione forms are depleted in blood of obese and type 1 diabetic children. *Pediatr Diabetes*. 2011;13(3):272–7.
 61. Atig F, Raffá M, Habib B-A, Kerkeni A, Saad A, Ajina M. Impact of seminal trace element and glutathione levels on semen quality of Tunisian infertile men. *BMC Urol*. 2012;12(1):6.
 62. Ochseedorf FR, Buhl R, Bästlein A, Beschmann H. Glutathione in spermatozoa and seminal plasma of infertile men. *Hum Reprod*. 1998;13(2):353–9.
 63. Rizza S, Filomeni G. Chronicles of a reductase: biochemistry, genetics and physio-pathological role of GSNOR. *Free Radic Biol Med*. 2017;110:19–30.
 64. Bátiz LF, De Blas GA, Michaut MA, Ramírez AR, Rodríguez F, Ratto MH, et al. Sperm from Hyh mice carrying a point mutation in α SNAP have a defect in acrosome reaction. *PLoS One*. 2009;4(3):e4963.
 65. De Blas GA, Roggero CM, Tomes CN, Mayorga LS. Dynamics of SNARE assembly and disassembly during sperm acrosomal exocytosis. *PLoS Biol*. 2005;3(10):e323.

66. Brahmaraaju M, Shoeb M, Laloraya M, Kumar PG. Spatio-temporal organization of Vam6P and SNAP on mouse spermatozoa and their involvement in sperm–zona pellucida interactions. *Biochem Biophys Res Commun*. 2004;318(1):148–55.
67. Hwang SR, O’Neill A, Bark S, Foulon T, Hook V. Secretory vesicle aminopeptidase B related to neuropeptide processing: molecular identification and subcellular localization to enkephalin- and NPY-containing chromaffin granules. *J Neurochem*. 2006;100(5):1340–50.
68. Cadel S, Foulon T, Viron A, Balogh A, Midol-Monnet S, Noël N, et al. Aminopeptidase B from the rat testis is a bifunctional enzyme structurally related to leukotriene-A(4)hydrolase. *Proc Natl Acad Sci U S A*. 1997;94(7):2963–8.
69. Subirán N, Candenás L, Pinto FM, Cejudo-Roman A, Agirregoitia E, Irazusta J. Autocrine regulation of human sperm motility by the met-enkephalin opioid peptide. *Fertil Steril*. 2012;98(3):617–25.e3.
70. Kubo H, Kotani M, Yamamoto Y, Hazato T. Involvement of sperm proteases in the binding of sperm to the vitelline envelope in *Xenopus laevis*. *Zool Sci*. 2008;25(1):80–7.
71. de Mateo S, Castillo J, Estanyol JM, Ballescà JL, Oliva R. Proteomic characterization of the human sperm nucleus. *Proteomics*. 2011;11(13):2714–26.
72. Razan AE, Marine P, Romain B, Guy L, Yasmina A, Vincent A, et al. LEM-domain proteins are lost during human spermiogenesis but BAF and BAF-L persist. *Reproduction*. 2017;154(4):387–401.
73. Tiffit KE, Segura-Totten M, Lee KK, Wilson KL. Barrier-to-autointegration factor-like (BAF-L): a proposed regulator of BAF. *Exp Cell Res*. 2006;312(4):478–87.
74. Samavat JMS, Natali IPD, Degl’Innocenti SMS, Filimberti EMS, Cantini GPD, Di Franco AMS, et al. Acrosome reaction is impaired in spermatozoa of obese men: a preliminary study. *Fertil Steril*. 2014;102(5):1274–81.e2.
75. Fan Y, Liu Y, Xue K, Gu G, Fan W, Xu Y, et al. Diet-induced obesity in male C57BL/6 mice decreases fertility as a consequence of disrupted blood-testis barrier. *PLoS One*. 2015;10(4).
76. Fullston T, McPherson NO, Owens JA, Kang WX, Sandeman LY, Lane M. Paternal obesity induces metabolic and sperm disturbances in male offspring that are exacerbated by their exposure to an “obesogenic” diet. *Physiol Rep*. 2015;3(3):e12336.
77. Binder NK, Hannan NJ, Gardner DK. Paternal diet-induced obesity retards early mouse embryo development, mitochondrial activity and pregnancy health. *PLoS One*. 2012;7(12).

Publisher’s note Springer Nature remains neutral with regard to jurisdictional claims in published maps and institutional affiliations.